Revista Brasileira de Ciência do Solo

Division – Soil Processes and Properties | Commission – Soil Mineralogy

Do Aggregate Size Classes of the Subsurface Soil Horizon Have Different Chemical/Mineralogical Properties?

Rolff Vladimir Mitton[(1)], Vander Freitas Melo[(2)*] and Volnei Pauletti[(2)]

[(1)] Universidade Federal do Paraná, Departamento de Solos e Engenharia Agrícola, Programa de Pós-Graduação em Ciência do Solo, Curitiba, Paraná, Brasil.
[(2)] Universidade Federal do Paraná, Departamento de Solos e Engenharia Agrícola, Curitiba, Paraná, Brasil.

ABSTRACT: Variations in chemical and mineralogical properties of a soil can occur at short vertical and horizontal distances. The objective of the present study was to evaluate the chemical and mineralogical soil properties of different aggregate classes from young (Ustrochrept) and highly weathered (Acrustox) soils from the state of Paraná, Brazil. Undisturbed blocks (0.20 ×0.20 ×0.20 m) of soils were separated into aggregate classes: Acrustox – 8.0-4.0 mm; 4-2 mm; 2.0-0.5 mm; 0.5-0.2 mm; and <0.2 mm; and Ustrochrept – 8.0-4.0 mm; 4.0-2.0 mm; 2.0-0.5 mm; and 0.5-0.2 mm. The exchangeable K contents showed an opposite behavior for the two soils: higher contents in the Acrustox for the larger aggregate classes and higher contents in the Ustrochrept for the smaller aggregate classes. The crystallographic characteristics of hematite and goethite were variable according to the aggregate class. The goethite in the 2-4-mm aggregate class is expected to exhibit the highest reactivity for the Ustrochrept: lower growth and a more elongated form of the crystals. The smallest aggregate class presented the lowest contents of kaolinite and gibbsite in the clay fraction. Gibbsite and kaolinite in the intermediate classes presented higher growth in both soils. The studied soils present different side-by-side environments (aggregate classes) for the exploration by the root system. This means that for the precise identification of the environments explored by the roots of a single plant, field sampling should consider the aggregate class, obtained from an undisturbed soil sample. However, this is impractical in agricultural practice.

Keywords: kaolinite, hematite, goethite, gibbsite, K reserve.

*** Corresponding author:**
E-mail: vanderfm@ufpr.br

Received: February 28, 2018
Approved: September 19, 2018

How to cite: Mitton RV, Melo VF, Pauletti V. Do aggregate size classes of the subsurface soil horizon have different chemical/mineralogical properties? Rev Bras Cienc Solo. 2019;43:e0180041.
https://doi.org/10.1590/18069657rbcs20180041

INTRODUCTION

The soil structure is considered as one of the most important soil properties from an agricultural point of view and is related to other fundamental properties in soil-plant relationships. The study of the soil structure in the morphological sense is purely descriptive, while from the physical point of view, it is functional (Tagar et al., 2016). The soil physical properties determined by the type, size, and degree of development of the aggregates depend heavily on the organic matter content and the proportions and crystallography of the minerals [mainly kaolinite (Kt), hematite (Hm), goethite (Gt), and gibbsite (Gb)] of the clay fraction, where the shape of the mineral will strongly influence the morphology of the aggregates, mainly in the B horizon (Melo et al., 2008; Almeida et al., 2014). Organic matter is determinant in the soil aggregation, but, as we have worked with the B horizons of the soils and our focus was to check mineralogy properties, we did not directly discuss the contents and characteristics of organic matter in the different aggregate classes.

The minerals Hm, Gt, and Gb have disorganizing effects on phyllosilicate minerals in the clay fraction, mainly Kt. Thus, the higher content of Fe and Al oxides will correspond to a higher degree of disorganization at the microscopic level and, consequently, a structure closer to the granular type (Ferreira et al., 1999). On the other hand, these authors also discussed the effect of Kt on the structure in the soils, assigning it to the face-to-face arrangement of the Kt to form a structure predominantly in blocks (Wilson et al., 2017). The type of the clay fraction has an effect not only on the aggregate size, but also on the external morphology of the aggregates. The reduction of the external roughness of the aggregates is favored by the higher Kt content in the clay fraction. The opposite effect has been verified for Fe and Al oxides (Melo et al., 2008).

The Kt under a humid tropical climate often has a low degree of crystallinity (Hughes and Brown, 1979; Singh and Gilkes, 1992), which determines a greater influence of the mineral in the aggregation process of the soil. There are different degrees of structural order/disorder, depending on the formation and ordering characteristics of the kaolinite layers (Melo and Wypych, 2009): a) events in the formation of the individual layers: i) dioctahedral layer: occurrence of additional empty octahedral positions, which should be occupied by Al (in the ideal dioctahedral configuration, every three positions, only one is empty); isomorphic substitution of Al^{3+} by Fe^{3+}; shortening of the layer size in the *c* direction by repulsion between neighboring Al^{3+} atoms (corrugation of the layer); ii) tetrahedral layer: rotation of Si tetrahedra, formation of the ditrigonal cavity and reduction of layer size in the *b* direction; b) events in the stacking of the tetrahedral and dioctahedral layers for 1:1 structure formation: unordered stacking in the *b* direction; unordered stacking in the *a* direction due to the repulsion of the Si^{4+} and Al^{3+} atoms, avoiding overlap in the adjacent layers; and c) interstratification with layers of 2:1 minerals. Several studies have identified the interstice of smectite (Ryan and Huertas, 2009; Hong et al., 2012) and the presence of Fe^{3+} in the dioctaedral layer in the Kt (Melo et al., 2001; Gilkes and Prakongkep, 2016).

Iron oxides are also important in the clay fraction, mainly in more weathered and well-drained soils (Colombo et al., 2014). The minerals Hm and Gt have different mineralogical characteristics, such as an isomorphic substitution level of Fe by Al within the mineral structure, a different crystallinity degree, and a different size and form of the mineral. The crystal-chemical attributes of Fe oxides are affected by weathering stages and biopedoclimatic conditions (Long et al., 2016).

A great variation in the minerals of the clay fraction can occur, with direct effects on the genesis of the structure of the soils, such as form, size, and stability of the aggregates. These relationships have been extensively studied. Therefore, our aim was to further investigate the soil aggregates and to determine the chemical and mineralogical properties of different aggregate classes at the same soil.

In addition to the secondary minerals, the variation in the primary mineral contents between the aggregate classes located side-by-side of a soil could define the nutrition of the plants in the medium and long terms. Among the cationic nutrients, K is the only one that presents non-exchangeable forms in the soil, which makes the study of the reserve of this nutrient more complex. For this reason, we selected K to evaluate the soil mineral reserve in different aggregate classes. The mineral reserve of K is strongly dependent on the nature of the parent material, the degree of soil development and mineralogy of soil fractions (Qiu et al., 2014). In this context, to have a great variation in this reserve, in the present study, a young soil (Ustrochrept), originated from rocks rich in K mineral sources (granite-gneiss), and a highly weathered soil (Acrustox), originated from rocks naturally poor in primary mineral sources of K (basalt), were selected. Potassium is present in the soil in several chemical forms: in solution as free ions and as ionic pair, sites of exchange of the organic matter and clay minerals, and a non-exchangeable form adsorbed specifically onto the vermiculite and onto the wedges of micas and in the primary minerals in the structural form (Blanchet et al., 2017). Although the soil solution and the exchangeable K forms are considered readily available to plants, they only represent a very small percentage (up to 2 %) of total K in the soil (Zörb et al., 2014). The K in the structural form is the most representative in the soil and is usually found in biotite (trioctaedralmica), muscovite (dioctaedral mica), and feldspars (Nabiollahy et al., 2006).

Due to the smaller diameter of the micropores, it can be expected that the mineral reserve of aggregates less than 0.105 mm (smaller class) would be more significant in terms of the nutrient content because it represents a more confined environment, where less leaching of silica and bases can occur. Thus, in practical terms, plant roots growing in a soil with different aggregate classes (undisturbed soil block of 0.20 m) could find various microenvironments in terms of fertility and nutrient reserves. It is therefore hypothesized that the aggregate classes located size-by-size have a different microenvironment in term of chemical and mineralogical properties. The objective of the present study was to evaluate the chemical soil properties and mineralogical characteristics of the clay fraction of different classes of aggregates of subsurface horizons from young (Ustrochrept) and highly weathered (Acrustox) soils from the state of Paraná, Brazil.

MATERIALS AND METHODS

Sampling area

Two soils from the state of Paraná, Brazil, with different degrees of development and parental material were selected. An Acrustox (basaltic rocks) was sampled in Cascavel (24° 58’ 12” S; 53° 25’ 59” W), and an Ustrochrept (granite/gneiss) was sampled in Curitiba Metropolitan Region (25° 33’ 56” S; 48° 56’ 14” W). The soil classification followed the analytical methods and morphological procedures of the U.S. Soil Taxonomy (Soil Survey Staff, 2014) and the Brazilian Soil Classification System (Santos et al., 2013). The depth of the B horizon of the Acrustox (highly weathered) and the Ustrochrept (young) was 2.15 and 0.31 m, respectively. The Ustrochrept was sampled in the Serra do Mar region. The local and regional relief is mountainous, with a slope of more than 40 %. The relief of the Oxisol (Acrustox) is slightly flat, with a slope of 4 %. The correspondent soil classes according to the Brazilian System of Soil Classification (Santos et al., 2013) are *Latossolo Vermelho Distroférrico típico* and *Cambissolo Húmico Distrófrico típico*, respectively.

Both soils were located at the top of the areas, and the profiles were formed directly from the weathering of the parent material (*in situ*). There was also no morphological evidence of lithologic discontinuity along the soil profiles. This choice is important to minimize the effect of sediment transport on the chemical and mineralogical diversity of the aggregate classes. The soils were sampled in areas free from anthropic interference and under environmental preservation. The vegetation of the Ustrochreptis Brazilian Atlantic Rainforest, while that of the Acrustox is Mixed Ombrophylous Forest.

A trench was opened in each soil type, and disturbed samples were collected from all soil horizons for soil classification (Soil Survey Staff, 2014; Santos et al., 2013). Subsequently, the surface horizon was thoroughly removed and three (replicates) undisturbed blocks of soil (0.20 × 0.20 × 0.20 m) were collected from the B horizon. As the main objective of this study was to evaluate the relation between chemical properties and mineralogy, it was decided to not collect the undisturbed sample from the A horizon to minimize the influence of organic matter on aggregate analysis. The evaluation of non-exchangeable and structural K forms associated with soil minerals (mineral reserve) would be influenced by the presence of K in the structure of organic matter, and the conclusions about the mineral reserve of horizon A would be compromised. In the sampled soils, even to a lesser extent, intense root growth was verified in the B horizons. Both soils have a clayey B horizon: 686 g kg^{-1} of clay for the Acrustox and 528 g kg^{-1} for the Ustrochrept.

Aggregate separation and characterization

The undisturbed soil samples were manually crushed in the field by applying a light pressure, thus causing minimal changes in the original structure, and were then wrapped for transport. After air drying, the samples were separated into different size clusters, using a sieve system attached to an orbital shaker (RETSCH K G/ 5657 Haan) with agitation for 10 min [dry aggregate stability - Donagema et al. (2011)]. The machine provided working speed options in a range from 0 to 10, and the highest speed (10) was used in this study. Both soils were separated into five aggregate classes, but for the Ustrochrept, the aggregates did not pass through the 0.2-mm sieve. Ustrochrept: 8-4, 4-2, 2-0.5, and 0.5-0.2 mm; Acrustox: 8-4, 4-2, 2-0.5, 0.5-0.2, and <0.2 mm. The soils had different proportions of each aggregate class (from larger to smaller): Ustrochrept - 27, 26, 24, and 23 %; Acrustox - 14, 15, 31, 25, and 15 %.

The chemical characterizations (Table 1) of the different aggregate classes was performed according to Donagema et al. (2011).

Forms of K of different aggregate classes

To evaluate the exchangeable K contents in the different aggregate classes, two extractants were used: Mehlich-1 (H_2SO_4 0.05 mol L^{-1} and HCl 0.025 mol L^{-1}) and ammonium oxalate 1 mol L^{-1} (Donagema et al., 2011). The contents of K were determined by flame photometry.

Table 1. Chemical characterization of different aggregate classes of soils

Soil	Aggregate class[(1)]	pH(H_2O)	Ca^{2+}	Mg^{2+}	H	K^+	Al^{3+}	$CEC_{pH7.0}$	TOC[(2)]	P
	mm		cmol$_c$ kg^{-1}						g kg^{-1}	mg kg^{-1}
Ustrochrept	8-4	4.00	0.10	0.07	9.76	0.03	3.34	13.2	5.6	14.1
Ustrochrept	4-2	4.01	0.20	0.08	9.72	0.03	3.38	13.3	16.7	6.5
Ustrochrept	2-0.5	4.00	0.20	0.07	9.73	0.03	3.37	13.3	7.8	10.7
Ustrochrept	0.5-0.2	4.06	0.40	0.20	8.95	0.04	3.15	12.7	4.6	24.0
Acrustox	8-4	3.91	0.40	0.10	11.45	0.05	2.65	14.6	19.0	20.2
Acrustox	4-2	3.88	0.30	0.09	11.53	0.05	2.57	14.4	21.3	6.8
Acrustox	2-0.5	3.85	0.30	0.07	11.68	0.04	2.42	14.4	14.5	18.9
Acrustox	0.5-0.2	3.86	0.30	0.10	11.47	0.04	2.63	14.4	17.9	10.5
Acrustox	<0.2	3.85	0.30	0.10	11.47	0.04	2.63	14.5	14.5	20.0

[(1)] For the Ustrochrept, aggregates did not pass the 0.2-mm sieve (only four classes of aggregates). [(2)] TOC = total organic carbon determined by the K-dichromate method. pH(H_2O) (soil: solution at a ratio of 1:2.5 v/v); non-exchangeable potential acidity (H) (calcium acetate 0.5 mol L^{-1}, pH 7); exchangeable Ca^{2+}, Mg^{2+}, and Al^{3+} (KCl 1 mol L^{-1}); available P and exchangeable K^+ (H_2SO_4 0.05 mol L^{-1} and HCl 0.025 mol L^{-1} - Mehlich-1). $CEC_{pH7.0}$ = $K^+ + Ca^{2+} + Mg^{2+} + Al^{3+} + H$.

For the non-exchangeable K, 0.3 g of aggregate samples were transferred to Teflon tubes in the presence of 5 mL of HNO_3 1 mol L^{-1} (Melo et al., 2016). The tubes were sealed and kept in a microwave oven (Mars Xpress 6, CEM) for 5 min and 30 s as the temperature reached 100 °C. This temperature was then maintained for an additional period of 4 min and 30 s.

For the total K, 0.3 g of the aggregate sample were placed in a sealed Teflon tube with 9 mL of concentrated HNO_3 and 3 mL of concentrated HF (EPA 3052 - Usepa, 1996). The tubes were subjected to microwave radiation (Mars Xpress 6, CEM) for 5 min and 30 s to reach 180 °C, attaining a maximum pressure of 16 atm for 4 min 30 s for their acid digestion at constant temperature and pressure.

Sand, silt, and clay fraction separation of different aggregate classes

The oxidation of organic compounds was performed by treating 20 g of aggregate with H_2O_2 (30 % v/v) in a water bath at 70 °C. The residue was dispersed in 0.2 mol L^{-1} of NaOH. The sand fraction was retained on a 0.053-mm sieve mesh, and silt and clay fractions were separated after sedimentation procedures, according to Stoke's law (Jackson, 1979).

To characterize the mineralogy of the fractions, samples of larger and smaller aggregate classes were analyzed by X-ray diffraction (XRD) (Table 2). The diffraction patterns (random powder mounts) were obtained in a Panalytical X´Pert3 device, with a speed of 0.42 °2θ s^{-1}, and analyzed in the 5-70 °2θ range. The diffractometer was equipped with a Ni filter, a graphite monochromator system, and used a CuKα radiation, operated at 40 kV and 40 mA.

Mineral predominance in silt and clay fractions was estimated based in peak height (intensity or number of counts) in the XRD pattern of each sample. In the sand fraction, quartz was the only observed mineral.

Short-range order iron oxides in the clay fraction of different aggregate classes

The short-range order Fe oxides of the clay fraction were extracted with a 0.2 mol L^{-1} ammonium oxalate, pH 3.0, in the dark (McKeague, 1978). The Fe content was determined in the extract via the orthophenanthroline colorimetric method (OCM) in a UV-Vis spectrophotometer at a wavelength of 510 nm.

Total pedogenetic Fe oxides in the clay fraction of different aggregate classes

To concentrate kaolinite and gibbsite and to study the composition of crystallized Fe oxides, the clay samples of the aggregate classes were submitted to dithionite-citrate-bicarbonate extraction (DCB) (Mehra and Jackson, 1960). The residue was washed with $(NH_4)_2CO_3$ 1 mol L^{-1} and deionized water, and the Fe content was determined in the extract by OCM.

Table 2. Mineralogy by X-ray diffraction of sand, silt, and clay fractions of the larger and smaller aggregate classes of soils

Soil	Aggregate class[(1)]	Sand	Silt		Clay	
			Main	Minor	Main	Minor
	mm					
Ustrochrept	8-4	Qz	Qz	Cl, Fp, Mi	Kt, Mi	Gb, Cl
Ustrochrept	0.5-0.2	Qz	Qz	Cl, Fp, Mi	Kt, Mi	Gb, Cl
Acrustox	8-4	Qz	Qz		Hm, Gb, Kt	
Acrustox	<0.2	Qz	Qz		Hm, Gb, Kt	

[(1)] For the Ustrochrept, aggregates did not pass the 0.2-mm sieve. Qz = Quartz; Gb = Gibbsite; Hm = Hematite; Cl = Chlorites; Fp = K-Feldspar; Mi = Mica; Kt = Kaolinite.

Extraction of gibbsite and kaolinite in the clay fraction of different aggregates classes

The clay samples of the aggregate classes were submitted to the extraction of kaolinite and gibbsite with boiling NaOH 5 mol L^{-1} (Norrish and Taylor, 1961). After washing to remove excess salts and subsequent drying, the residue was analyzed via XRD.

Investigation of kaolinite and gibbsite from the DCB residue of different aggregates classes

A sample of 15 mg of Fe-free clay was placed on the platinum crucible of the differential thermogravimetric analyzer and was gradually heated from room temperature to 950 °C, using a nitrogen atmosphere at a heating rate of 10 °C min^{-1} and a gas flow of 50 mL min^{-1}. The identification in the thermograms was based on the position of the major dehydroxylation peaks of kaolinite and gibbsite. The measurement of mass loss of the gibbsite was facilitated by the previous removal of the goethite by the DCB method. The kaolinite and gibbsite contents were determined by considering the mass loss via heating of each sample. The gibbsite and kaolinite contents in the DCB residue were corrected for the untreated clay by considering the mass loss of the sample with DCB extraction.

The crystallite sizes of kaolinite and gibbsite were calculated from the width at half height of the reflections (001) and (002), respectively, using NaCl as the internal standard in the XRD patterns (Klug and Alexander, 1954; Melo et al., 2001).

The crystallinity index (Hughes and Brown Crystallinity Index) for kaolinite was calculated only in the Ustrochrept. Due to the high contents of gibbsite in the clay samples of the Acrustox, the crystallinity of kaolinite was not estimated via XRD. The reflection (110) of the gibbsite at 20.3 °2θ (CuKα radiation) makes it impossible to measure the parameter h1 of the equation proposed by Hughes and Brown (1979).

Study of the Fe oxides by XRD in the extraction residue with NaOH 5 mol L^{-1} of different aggregate classes

The ratio of goethite (Gt)/hematite (Hm) was calculated using the equation proposed in Resende et al. (1987): $[Gt/(Gt + Hm)] = 1- \{4 \times A(Hm_{012})/[4 \times A(Hm_{012)} + A(Gt_{110})]\}$. In which $A(Hm_{012})$ is the area of the 012 reflection of the hematite; and $A(Gt_{110})$ is the area of the 110 reflection of the goethite.

The isomorphic substitution of Fe by Al in the structure of Fe oxide minerals was estimated by the reflection of the peak position in the XRD patterns. The scan seed was reduced to 0.10 °2θ s^{-1} to improve the Fe oxide counts; the XRD range was sustained at 5-70 °2θ.

For the hematite, the Al-substitution was calculated with the equation proposed in Schulze (1984), while for the goethite, we used the equation proposed in Schwertmann et al. (1979).

Statistical analysis

All analyses, except XRD, were performed in triplicate. Analysis of variance (two-way ANOVA) was performed at 5 % probability level ($p<0.05$). The data were submitted to the comparison of means by the Duncan test (5 %) through the following programs: Statistica 10.0, Sigma Plot 12.0, and Microsoft Office Excel 2016.

RESULTS AND DISCUSSION

Forms of K in different aggregate classes

The content of K extracted by Mehlich-1 for the Ustrochrept throughout the aggregates varied widely, with a mean value of 15.7 mg kg^{-1} (Figure 1a). The highest K content

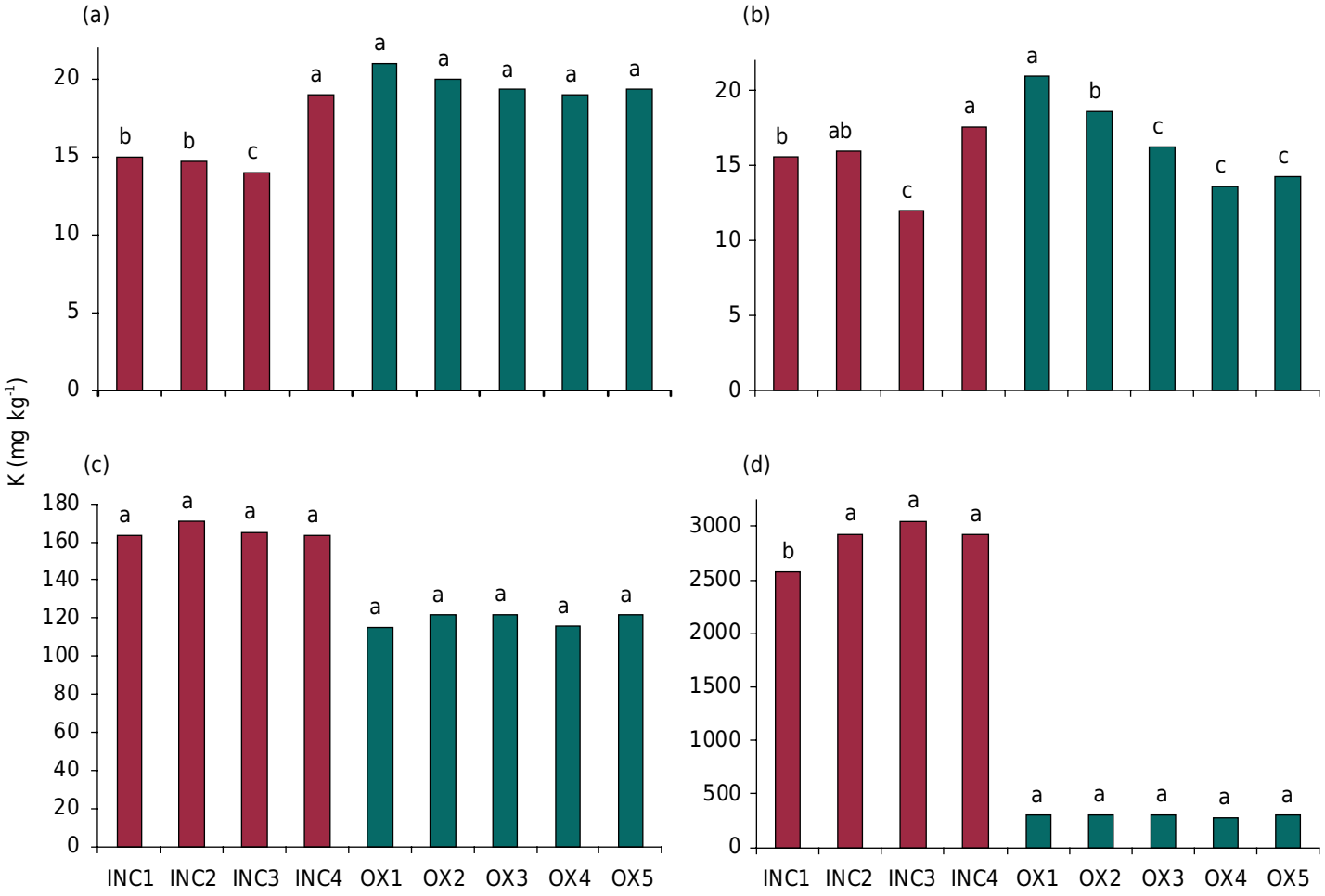

Figure 1. Contents of K in different forms of aggregate samples: Mehlich-1 (a), NH_4Oac (b), HNO_3 (c), and HF/HNO_3 (d). INC = Ustrochrept; OX = Acrustox; INC1 = 8-4 mm; INC2 = 4-2 mm; INC3 = 2-0.5 mm; INC4 = 0.5-0.2 mm; OX1 = 8-4 mm; OX2 = 4-2 mm; OX3 = 2-0.5 mm; OX4 = 0.5-0.2 mm; OX5 = <0.2 mm. Comparisons of the means are made only for the aggregates of the same soil.

(20.8 mg kg^{-1}) was observed in the smallest aggregates (0.5-0.2 mm). The Acrustox presented similar values, with a mean value of 19.8 mg kg^{-1} within the aggregates.

Via NH_4Oac, the exchangeable K is determined, but also a portion of the non-exchangeable K (Sarkar et al., 2013). Due to the proximity of ionic radiuses (0.13 nm) between K^+ and NH_4^+, there is the possibility of exchanging these ions at K^+-specific adsorption sites (Rao and Srinivas, 2017). In the samples of the Ustrochrept, the behavior between the aggregate classes and the contents of K extracted by NH_4Oac were similar to the results of the extraction with Mehlich-1 (Figure 1b). There was an intensification of the differences between the K-NH_4Oac contents in the different aggregate classes of the Acrustox. Unlike the Ustrochrept, the larger aggregate classes of the Acrustox had higher contents of K-NH_4Oac. Therefore, there was no consistent behavior between the two soils in terms of increases or decreases in exchangeable K contents towards the larger or smaller aggregates. The distribution of exchangeable K in the aggregate classes was random, but with significant differences. It can be stated that the soil itself, in general, presents different side-by-side environments for the exploration by the root system. Other studies concerning chemical, physical, and biological properties of the different aggregate size class have already shown the heterogeneity of the soil matrix: i) biological and organic matter contents in an AquiticPaleudalf from the Garden plots at IACR-Rothamsted (Ashman et al., 2003); ii) organic C and total microbial C of a Gleyic Cambisol from Stuttgart-Hohenheim (Dorodnikov et al., 2009); iii) glycoprotein produced on hyphae and spores of arbuscular mycorrhizal (AM) fungi in an Ultisol in the Mid-Atlantic area of the U.S. (Wright et al., 2007).

The contents of non-exchangeable K (HNO_3) were similar among the aggregates of the Ustrochrept and the Acrustox (Figure 1c). Following the non-exchangeable content, the content of structural K was higher in the Ustrochrept than in the Acrustox (Figure 1d). This indicates that the weathering processes are far more advanced in the Acrustox than the Ustrochrept. Mineral sources of K reserves, such as micas and K-feldspar, were identified in the clay and silt fractions for the Ustrochrept (Table 2). The mineralogy of the soil fraction is compatible with the granite/gneiss mineralogy. In the young soil (Ustrochrept), the rock minerals were preserved in the soil fraction.

In the Ustrochrept, the largest class of aggregate presented a lower total K content, while the other classes presented similar contents. The Acrustox presented a steadier content among its aggregates. The pedobioturbation processes are more intense in the Acrustox, which promotes greater homogenization of the soil matrix mineralogy.

Iron oxides in the clay fractions of different aggregate classes

The content of short-range order Fe (ammonium oxalate - AO) for the Ustrochrept varied from 5.1 to 5.6 g kg^{-1}, while for the Acrustox, it ranged from 2.9 to 3.0 g kg^{-1}, according to the aggregate classes (Figure 2a). The high content of short-range order Fe oxides of the Ustrochrept is compatible with the low development degree of this soil and with its parent material. The only significant difference in the Fe-AO content among the aggregate classes was the lowest content for the 2-4-mm class in the Ustrochrept. This aggregate class had the highest organic carbon content for the Ustrochrept (Table 1). Organic matter slows down the crystallization of Fe oxides and favors the stability of short-range order forms such as ferrihydrite (Kämpf and Schwertmann, 1983; Poggere et al., 2016). The short-range order Fe oxides present a high specific surface area and activity in the soil (Simas et al., 2006; Mendonça et al., 2013). For the Acrustox, this tendency was not found, and all aggregates showed a similar concentration of Fe-OA.

In contrast to the Fe-AO content, the Acrustox presented a higher variation in Fe-dithionite-citrate-bicarbonate (DCB) contents (Figure 2b). The basalt parent material may have induced greater variations in the total pedogenic Fe content throughout the Acrustox aggregate classes. In the Ustrochrept, however, granite has a lower content of mafic minerals and thus a lower influence on the distribution of these minerals in the different aggregate classes. As observed for the K contents, there was no consistent variation in the Fe-DCB contents towards the larger or smaller aggregate classes.

Hematite (Hm) and goethite (Gt) were the only Fe oxide minerals in the clay fraction treated with NaOH 5 mol L^{-1} in the XRD patterns. Hematite peaks were not observed in the clay fraction for the Ustrochrept, and the ratio of Gt/(Gt+Hm) was 1.0 in all aggregate classes (Table 3). The main factors that favor the formation of Gt and increase the Gt/(Gt+Hm) ratio are: lower iron content in the parental material, lower temperatures, higher humidity and organic matter and lower pH values (Schwertmann and Kämpf, 1985). The Acrustox presented reflections of both Hm and Gt. The ratio Gt/(Gt+Hm) in all aggregate classes for the Acrustox was lower than 0.3 (Table 3), therefore proving the predominance of Hm.

The Gt/(Gt+Hm) ratio was similar between the different aggregate classes for both soils (Table 3), indicating that the pedogenetic conditions for hematite and goethite formation were the same for the entire soil matrix. In the 4-2-mm aggregate class of the Acrustox, there was a higher content of pedogenic oxides (Figure 2b), but there was no variation in the Gt/(Gt + Hm) ratio in relation to the other aggregate classes (Table 3).

The Gt crystallite size at (130) and (111) for Ustrochrept and the Hm (012) for the Acrustox were different among the different aggregate classes, indicating that the growth

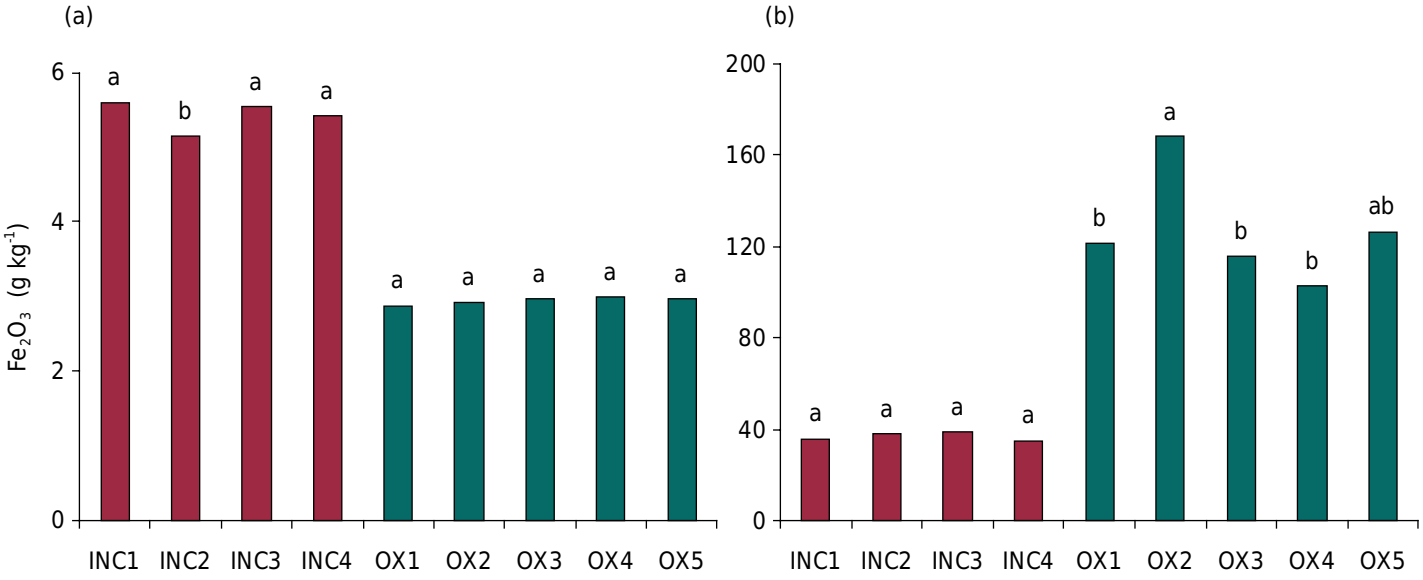

Figure 2. Contents of Fe oxides in the clay fraction extracted by different methods: ammonium oxalate (a) and dithionite-citrate-bicarbonate (b). INC1 = 8-4 mm; INC2 = 4-2 mm; INC3 = 2-0.5 mm; INC4 = 0.5-0.2 mm; OX1 = 8-4 mm; OX2 = 4-2 mm; OX3 = 2-0.5 mm; OX4 = 0.5-0.2 mm; OX5 = <0.2 mm. Comparisons of the means are made only for the aggregates of the same soil.

of Fe oxides in these planes in the clay fraction was differentiated within the same soil matrix. The smaller the crystal size, the greater its specific surface area and the greater its reactivity in the soil (Schwertmann and Kämpf, 1985).

However, the relationship between the size of the crystallites in the various directions of Fe oxides was similar among the different aggregate classes, especially for Hm (Table 3). Relations closer to 1.0 indicate a more isodimensional morphology of the crystals, with a lower surface area exposure. On the other hand, very distant values of 1.0 are consistent with a more acicular form of Gt (Ristić et al., 2013).

The isomorphic substitution (IS) in the Ustrochrept was determined only in the Gt, since there was no detection of Hm in any of the aggregate classes of this soil. For the Acrustox, the substitution was evaluated only in the Hm, since the Gt reflection for the peak (111) presented a very low intensity. In the Ustrochrept, the Al-substitution in the Gt varied from 231.4 to 273.8 mmol mol^{-1} among the aggregates, with a higher value in the 2-4-mm aggregate class (Table 3). Therefore, Gt in the 2-4-mm aggregate size is expected to exhibit the highest reactivity for the Ustrochrept: the ratio between crystallite size farthest from 1.0 (ratio A = 3.0) and lower mean crystal sizes in the directions (110) and (111), as well as a high isomorphic substitution of Fe for Al.

For the Acrustox, the Al-substitution in the Hm was higher for the 2-0.5-mm aggregate size. The isomorphic substitution of Fe by Al (IS) in the structure of Gt and Hm is quite common, and as a result causes changes in cell unit size and particle crystallinity. The higher IS degree in Fe oxides is usually associated with more weathered soils with higher Al activity.

Kaolinite (Kt) and gibbsite (Gb) in the clay fractions of different aggregate classes

There were significant differences in the contents of Gb and Kt in the clay fractions as a function of the Ustrochrept and Acrustox aggregate classes (Figure 3). In the Acrustox, the class <0.2 mm presented the lowest contents of Gb and Kt. It is possible that the smaller size of this aggregate provides greater water retention in a micro-type environment. For example, in soils from northern Thailand, the formation of Gb was

Table 3. Crystallographic parameters of hematite (Hm) and goethite (Gt) in the clay fractions of different aggregate classes of soils

Soil	Aggregate class[1]	Gt/(Gt + Hm)	Crystallite size						Crystallite size ratio[2]			Isomorphic substitution		WHI Gt (110)[3]
			Gt (110)	Gt (130)	Gt (111)	Hm (104)	Hm (012)	Hm (110)	A	B	C	Gt	Hm	
	mm		nm									mmol mol^{-1}		°2θ
Ustrochrept	8-4	1.0 a	18.1 a	12.5 ab	7.6 a	-	-	-	2.4 b	1.5 a	-	231 b	-	0.5 a
Ustrochrept	4-2	1.0 a	17.3 a	13.4 a	5.7 b	-	-	-	3.0 a	1.3 a	-	273 a	-	0.5 a
Ustrochrept	2-0.5	1.0 a	18.5 a	11.8 b	7.8 a	-	-	-	2.4 b	1.6 a	-	248 b	-	0.4 a
Ustrochrept	0.5-0.2	1.0 a	17.5 a	11.1 b	7.3 a	-	-	-	2.4 b	1.6 a	-	258 ab	-	0.5 a
Acrustox	8-4	0.2 a	9.0 a	-	-	10.6 a	17.1 a	19.1 a	-	-	0.6 a	-	192 c	0.9 a
Acrustox	4-2	0.3 a	7.9 a	-	-	10.7 a	16.2 a	16.5 a	-	-	0.7 a	-	202 c	1.0 a
Acrustox	2-0.5	0.2 a	8.9 a	-	-	11.5 a	13.4 b	18.4 a	-	-	0.6 a	-	281 a	0.9 a
Acrustox	0.5-0.2	0.2 a	8.8 a	-	-	11.8 a	15.6 ab	16.9 a	-	-	0.7 a	-	248 ab	0.9 a
Acrustox	<0.2	0.2 a	9.5 a	-	-	11.9 a	14.0 b	17.2 a	-	-	0.7 a	-	267 b	0.9 a

[1] For the Ustrochrept, the aggregates did not pass the 0.2-mm sieve (only four classes of aggregates). [2] Crystallite size ratio: A = Gt (110)/Gt (111); B = Gt (110)/Gt (130); C = Hm (104)/Hm (110). [3] WHI = width at half intensity of the reflection. - = not determined due to the absence or the low intensity of the mineral in the reflection by XRD. Comparisons of the means are made only for the aggregates of the same soil.

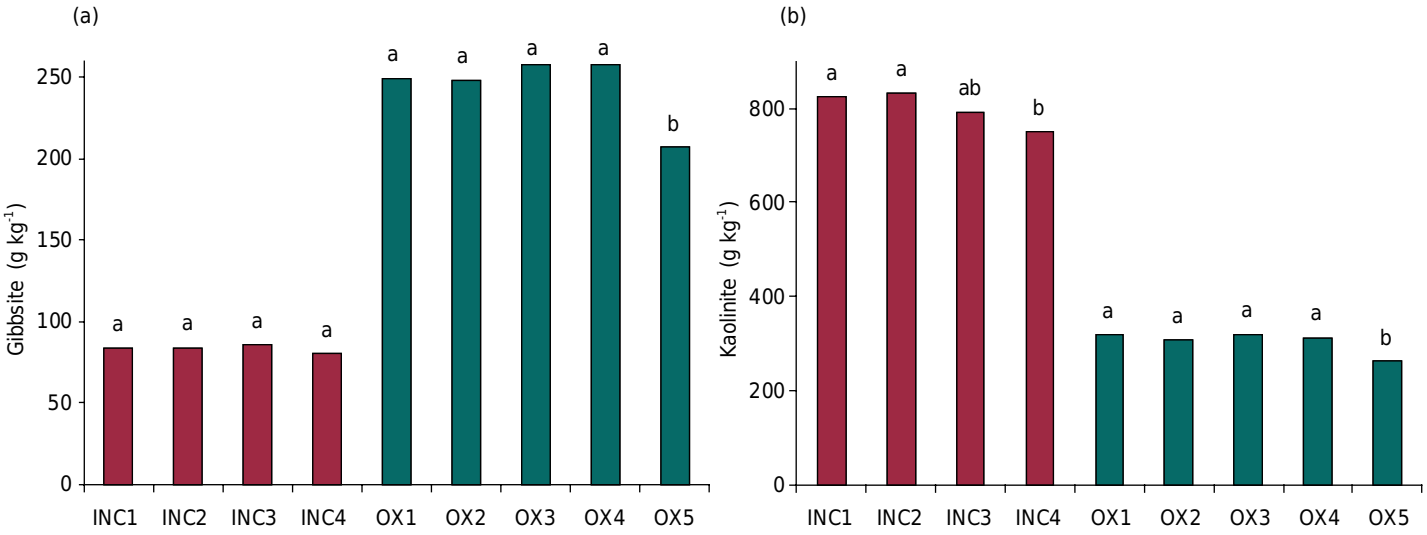

Figure 3. Contents of gibbsite and kaolinite in the clay fraction of different classes of aggregates of Ustrochrept and Acrustox. INC1 = 8-4 mm; INC2 = 4-2 mm; INC3 = 2-0.5 mm; INC4 = 0.5-0.2 mm; OX1 = 8-4 mm; OX2 = 4-2 mm; OX3 = 2-0.5 mm; OX4 = 0.5-0.2 mm; OX5 = <0.2 mm. Comparisons of the means are made only for the aggregates of the same soil.

not only dependent on the parent material, but also on the water storage capacity (Herrmann et al., 2007). The greater the water storage capacity, the lower the likelihood of Gb formation. In the Ustrochrept, the smaller aggregate class also had the lowest Kt contents. Greater water retention within the aggregate should reduce the desilication process and decrease the stability of minerals with a lower molar ratio of Si to Al (0:1 - Gb and 1:1 - Kt).

The variation in the contents of secondary minerals in aggregate classes of the soil defines the formation of micro-environments with different chemical properties. For example, the lower Gb contents in the aggregate class <0.2 mm in the Acrustox (Figure 3) is compatible with the lower specific adsorption of P, ensuring plant availability. Commonly, a binder exchange between the aluminol group (-AlOH) and the $H_2PO_4^-$ molecule occurs, resulting in the formation of internal sphere binding with a strong covalent character (Gérard, 2016). The lower contents of Gb also reduces AEC (anion exchange capacity) and the

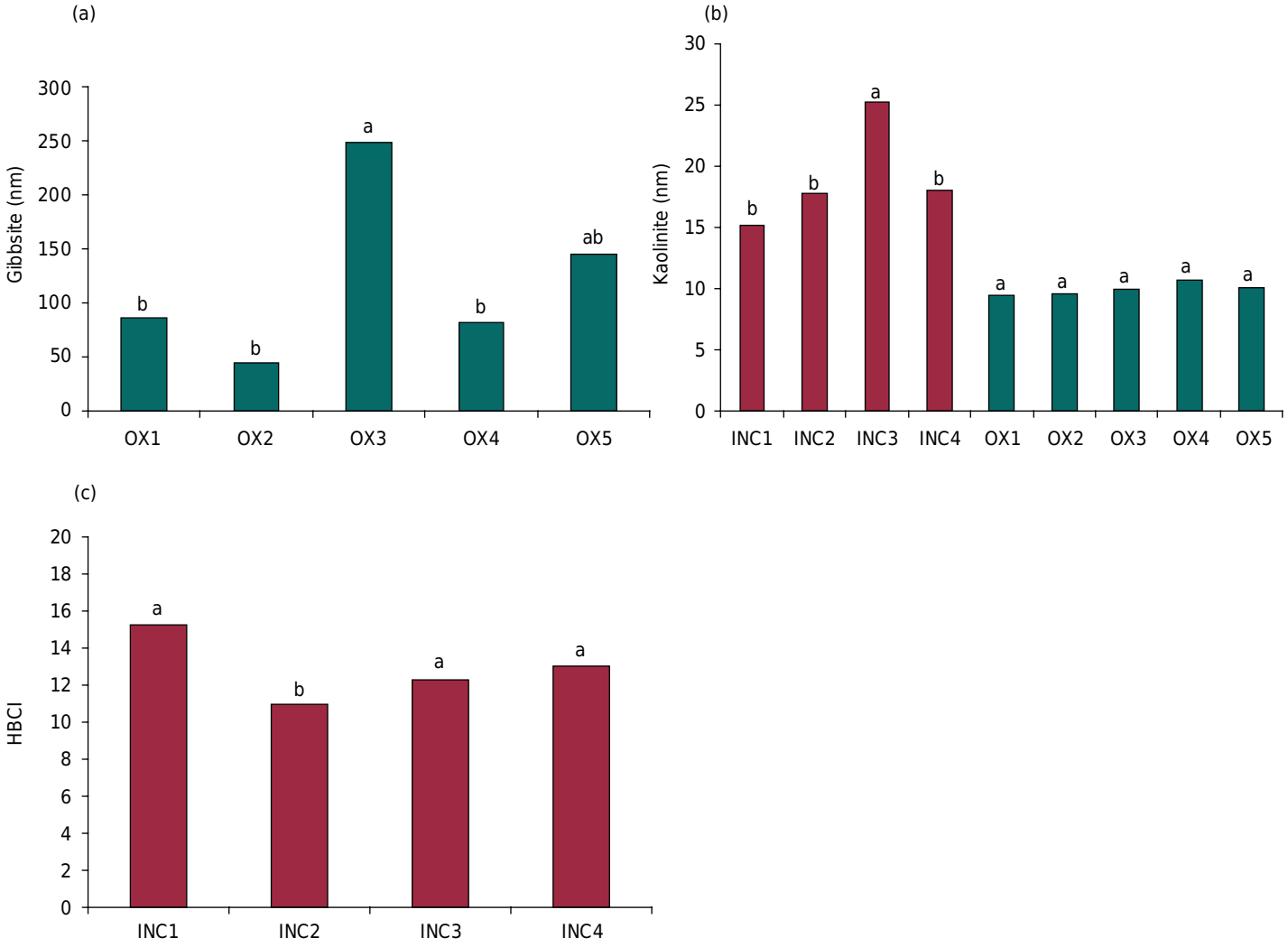

Figure 4. Crystallite size of gibbsite in the plane (002) (a), of kaolinite in the plane (001) (b), and Hughes and Brown Crystallinity Index of kaolinite (c). INC1 = 8-4 mm; INC2 = 4-2 mm; INC3 = 2-0.5 mm; INC4 = 0.5-0.2 mm; OX1 = 8-4 mm; OX2 = 4-2 mm; OX3 = 2.0-0.5 mm; OX4 = 0.5-0.2 mm; OX5 = <0.2 mm. Comparisons of the means are made only for the aggregates of the same soil.

adsorption of anionic nutrients, such as SO_4^{2-} and NO_3^-, since the Al-OH group is a weak acid whose pH value of the zero-charge point is between 8 and 9 (Poggere et al., 2016). However, these effects need to be confirmed in future studies, including the cultivation of plants in different classes of soil aggregates.

There was no formation of aggregates smaller than 0.2 mm in the Ustrochrept. Considering the last class of aggregates of the Ustrochrept (0.5-0.2 mm) and the last two classes of Acrustox (0.5-0.2 mm and <0.2 mm), the following average amounts of aggregates were obtained: Ustrochrept – 23 % and Acrustox – 40 %. The mean values of Fe oxides (Hm) (Figure 2, Table 3) and Gb (Figure 3) in the Acrustox were more than twice as high as that of the Ustrochrept, confirming the effects of these minerals on the formation of more isodimensional and small structures. The minerals Hm, Gb, and Gt interfere in the face-to-face adjustment of phyllosilicate minerals (disorganizing effect) such as Kt, which favors the formation of smaller structures with a spherical shape in the B horizon of highly weathered soils (Melo et al., 2008; Wilson et al., 2017).

The values of the crystallite size of Gb (002) varied from 87 to 249 nm, with significant differences between aggregate classes (Figure 4a). There was higher growth of the mineral in the intermediate aggregate class (2-0.5 mm). The aggregate classes of 2-0.5 mm and <0.2 mm presented the lowest contents of organic carbon (Table 1). Organic matter

interferes negatively with the growth of mineral crystals (Melo et al., 2001); however, the difference in crystal size cannot be credited to organic matter alone, since the formation and stabilization of aggregates is a slow process (pedological time), and the chemical properties of the aggregates must change over time.

The crystallite size of the Kt in the Ustrochrept is, on average, almost twice as high as that of the Acrustox (Figure 4b). The higher the Kt content in the clay fraction, the higher the crystallite growth (Melo et al., 2001). Kaolinite growth in soils can also be affected by the degree of soil weathering, mixed-layering with other phyllosilicate minerals, climatic conditions, and the influence of inorganic and organic ions in the soil solution (Singh and Gilkes, 1992). Apparently, the high pedogenetic Fe_2O_3 contents in the Acrustox had a negative influence on kaolinite growth. There was no significant difference in crystallite size between the aggregates of the Acrustox. For the Ustrochrept, all aggregates except those of 2.0-0.5 mm were statistically equal.

The Ustrochrept presented a Hughes and Brown Crystallinity Index (HBCI) from 12.4 to 15.4, with an average of 13.0. The aggregate size 4-2 mm presented a lower crystallinity when compared to the other aggregate classes of the Ustrochrept (Figure 4c). There was no apparent relationship between crystallite size and the HBCI value. The opposite behavior has also been found (Chittleborough and Walker, 1988), in which the crystallinity of the Kt was higher in the larger crystallites. The HBCI of the Ustrochrept was relatively high. The median values of 5.4 and 5.8 were reported for Kt from western (Koppi and Skjemstad, 1981) and eastern Australian soils (Singh and Gilkes, 1992). The HBCI values, however, are lower than the standard Kt, e.g., values between 38 to 83 were found for standard kaolinites including Georgia kaolinite (Hughes and Brown, 1979; Singh and Gilkes, 1992). Although the HBCI is an empirical index and provides no information about the structural defects, it is extremely useful in ranking soil Kt based on structural disorders and shows relationships with other properties of Kt, representing a function of crystal order (Melo et al., 2001).

CONCLUSIONS

The distribution of exchangeable K in the different aggregate classes was random, but with significant differences. The selected soils present different side-by-side environments for the exploration of the root system. The more stable forms of K (non-exchangeable and structural) were more homogeneous among the different classes of aggregates, especially for the more weathered soil.

The aggregates of Ustrochrept (*Cambissolo Húmico Distrófrico típico*) and Acrustox (*Latossolo Vermelho Distroférrico típico*) presented different chemical environments when considering crystalline Fe oxides. The crystallographic characteristics of hematite and goethite were variable according to the aggregate class. The goethite in the 2-4-mm aggregate class is expected to exhibit the highest reactivity for the Ustrochrept: less growth and a more elongated form of the crystals.

The smaller aggregate classes presented the lowest contents of kaolinite and gibbsite in the clay fraction. Gibbsite and kaolinite in the intermediate classes of aggregates in Acrustox and Ustrochrept, respectively, presented higher growth.

REFERENCES

Almeida RF, Machado HA, Martins FP, Queiroz IDS, Teixeira WG, Mikhael JER, Borges EN. Correlação do tamanho e distribuição dos agregados em Latossolos Amarelo da região do Triângulo Mineiro em diferentes ambientes. Biosci J. 2014;30:1325-34.

Ashman MR, Hallett PD, Brookes PC. Are the links between soil aggregate size class, soil organic matter and respiration rate artefacts of the fractionation procedure? Soil Biol Biochem. 2003;35:435-44. https://doi.org/10.1016/S0038-0717(02)00295-X

Blanchet G, Libohova Z, Joost S, Rossier N, Schneider A, Jeangros B, Sinaj S. Spatial variability of potassium in agricultural soils of the canton of Fribourg, Switzerland. Geoderma. 2017;290:107-21. https://doi.org/10.1016/j.geoderma.2016.12.002

Gérard F. Clay minerals, iron/aluminum oxides, and their contribution to phosphate sorption in soils - a myth revisited. Geoderma. 2016;262:213-26. https://doi.org/10.1016/j.geoderma.2015.08.036

Chittleborough DJ, Walker PH. Crystallinity of soil kaolinites in relation to clay particle-size and soil age. Eur J Soil Sci.1988;39:81-6. https://doi.org/10.1111/j.1365-2389.1988.tb01196.x

Colombo C, Palumbo G, He J-Z, Pinton R, Cesco S. Review on iron availability in soil: interaction of Fe minerals, plants, and microbes. J Soil Sediment. 2014;14:538-48. https://doi.org/10.1007/s11368-013-0814-z

Donagema GK, Campos DVB, Calderano SB, Teixeira WG, Viana JHM. Manual de métodos de análise do solo. 2. ed. rev. Rio de Janeiro: Embrapa Solos; 2011.

Dorodnikov M, Blagodatskaya E, Blagodatsky S, Marhan S, Fangmeier A, Kuzyakov Y. Stimulation of microbial extracellular enzyme activities by elevated CO_2 depends on soil aggregate size. Glob Change Biol. 2009;15:1603-14. https://doi.org/10.1111/j.1365-2486.2009.01844.x

Ferreira MM, Fernandes B, Curi N. Mineralogia da fração argila e estrutura de Latossolos da região sudeste do Brasil. Rev Bras Cienc Solo. 1999;23:507-14. https://doi.org/10.1590/S0100-06831999000300003

Gilkes RJ, Prakongkep N. How the unique properties of soil kaolin affect the fertility of tropical soils. Appl Clay Sci. 2016;131:100-6. https://doi.org/10.1016/j.clay.2016.01.007

Herrmann L, Anongrak N, Zarei M, Schuler U, Spohrer K. Factors and processes of gibbsite formation in Northern Thailand. Catena. 2007;71:279-91. https://doi.org/10.1016/j.catena.2007.01.007

Hong H, Churchman GJ, Gu Y, Yin K, Wang C. Kaolinite-smectite mixed-layer clays in the Jiujiang red soils and their climate significance. Geoderma. 2012;173-174:75-83. https://doi.org/10.1016/j.geoderma.2011.12.006

Hughes JC, Brown G. A crystallinity index for soil kaolins and its relation to parent rock, climate and soil maturity. Eur J Soil Sci. 1979;30:557-63. https://doi.org/10.1111/j.1365-2389.1979.tb01009.x

Jackson ML. Soil chemical analysis: advanced course. Madison: Parallel Press; 1979.

Kämpf N, Schwertmann U. Goethite and hematite in a climosequence in southern Brazil and their application in classification of kaolinitic soils. Geoderma. 1983;29:27-39. https://doi.org/10.1016/0016-7061(83)90028-9

Klug HP, Alexander LE. X-ray diffraction procedures for polycrystalline and amorphous materials. New York: John Wiley & Sons; 1954.

Koppi AJ, Skjemstad JO. Soil kaolins and their genetic relationships in southeast Queensland, Australia. Eur J Soil Sci. 1981;32:661-72. https://doi.org/10.1111/j.1365-2389.1981.tb01738.x

Long X, Ji J, Barrón V, Torrent J. Climatic thresholds for pedogenic iron oxides under aerobic conditions: processes and their significance in paleoclimate reconstruction. Quaternary Sci Rev. 2016;150:264-77. https://doi.org/10.1016/j.quascirev.2016.08.031

McKeague JA. Manual on soil sampling and methods of analysis. Ottawa: Canadian Society of Soil Science; 1978.

Mehra OP, Jackson ML. Iron oxide removal from soils and clays by a dithionite-citrate system buffered with sodium bicarbonate. Clay Clay Miner. 1960;7:317-27. https://doi.org/10.1016/B978-0-08-009235-5.50026-7

Melo VF, Batista AH, Gilkes RJ, Rate AW. Relationship between heavy metals and minerals extracted from soil clay by standard and novel acid extraction procedures. Environ Monit Assess. 2016;188:668. https://doi.org/10.1007/s10661-016-5690-8

Melo VF, Moura R, Toledo FH, Lima VC, Ghidin AA. Morfologia de agregados de Latossolos bruno e vermelho do estado do Paraná, avaliada por imagens obtidas em *Scanner*. Rev Bras Cienc Solo. 2008;32:85-99. https://doi.org/10.1590/S0100-06832008000100009

Melo VF, Singh B, Schaefer CEGR, Novais RF, Fontes MPF. Chemical and mineralogical properties of kaolinite-rich Brazilian soils. Soil Sci Soc Am J. 2001;65:1324-33. https://doi.org/10.2136/sssaj2001.6541324x

Melo VF, Wypych F. Caulinita e Haloisita. In: Melo VF, Alleoni LRF, editores. Química e mineralogia do solo. Viçosa, MG: Sociedade Brasileira de Ciência do Solo; 2009. Pt 1. p. 427-504.

Mendonça T, Melo VF, Alleoni LRF, Schaefer CEGR, Michel RFM. Lead adsorption in the clay fraction of two soil profiles from Fildes Peninsula, King George Island. Antarct Sci. 2013;25:389-96. https://doi.org/10.1017/S0954102012001071

Nabiollahy K, Khormali F, Bazargan K, Ayoubi Sh. Forms of K as a function of clay mineralogy and soil development. Clay Miner. 2006;41:739-49. https://doi.org/10.1180/0009855064130216

Norrish K, Taylor RM. The isomorphous replacement of iron by aluminium in soil goethites. Eur J Soil Sci. 1961;12:294-306. https://doi.org/10.1111/j.1365-2389.1961.tb00919.x

Poggere GC, Melo VF, Francelino MR, Schaefer CE, Simas FN. Characterization of products of the early stages of pedogenesis in ornithogenic soil from Maritime Antarctica. Eur J Soil Sci. 2016;67:70-8. https://doi.org/10.1111/ejss.12307

Qiu S, Xie J, Zhao S, Xu X, Hou Y, Wang X, Zhou W, He P, Johnston AM, Christie P, Jin J. Long-term effects of potassium fertilization on yield, efficiency, and soil fertility status in a rain-fed maize system in northeast China. Field Crops Res. 2014;163:1-9. https://doi.org/10.1016/j.fcr.2014.09.017

Rao CS, Srinivas K. Potassium dynamics and role of non-exchangeable potassium in crop nutrition. Indian J Fertil. 2017;13:80-94.

Resende M, Bahia Filho AFC, Braga JM. Mineralogia da argila de Latossolos estimada por alocação a partir do teor total de óxidos do ataque sulfúrico. Rev Bras Cienc Solo. 1987;11:7-23.

Ristić M, Opačak I, Musić S. The synthesis and microstructure of goethite particles precipitated in highly alkaline media. J Alloy Compd. 2013;559:49-56. https://doi.org/10.1016/j.jallcom.2013.01.027

Ryan PC, Huertas FJ. The temporal evolution of pedogenic Fe-smectite to Fe-kaolin via interstratified kaolin-smectite in a moist tropical soil chronosequence. Geoderma. 2009;151:1-15. https://doi.org/10.1016/j.geoderma.2009.03.010

Santos HG, Jacomine PKT, Anjos LHC, Oliveira VA, Oliveira JB, Coelho MR, Lumbreras JF, Cunha TJF. Sistema brasileiro de classificação de solos. 3. ed. rev. ampl. Rio de Janeiro: Embrapa Solos; 2013.

Sarkar GK, Chattopadhyay AP, Sanyal SK. Release pattern of non-exchangeable potassium reserves in Alfisols, Inceptisols and Entisols of West Bengal, India. Geoderma. 2013;207-208:8-14. https://doi.org/10.1016/j.geoderma.2013.04.029

Schulze DG. The influence of aluminium on iron oxides. VIII. Unit-cell dimensions of Al-substituted goethites and estimation of Al from them. Clay Clay Miner. 1984;32:36-44.

Schwertmann U, Fitzpatrick RW, Taylor RM, Lewis DG. The influence of aluminium on iron oxides. Part II. Preparation and properties of Al-substituted hematites. Clay Clay Miner. 1979;29:269-76.

Schwertmann U, Kämpf N. Properties of goethite and hematite in kaolinitic soils of southern and central Brazil. Soil Sci. 1985;139:344-50.

Simas FNB, Schaefer CEGR, Melo VF, Guerra MBB, Saunders M, Gilkes RJ. Clay sized minerals in permafrost-affected soils (Cryosols) from King George Island, Antarctica. Clay Clay Miner. 2006;54:721-36. https://doi.org/10.1346/CCMN.2006.0540607

Singh B, Gilkes RJ. Properties of soil kaolinites from south-westen Australia. Eur J Soil Sci. 1992;43:645-67. https://doi.org/10.1111/j.1365-2389.1992.tb00165.x

Soil Survey Staff. Keys to Soil Taxonomy. 12th ed. Washington, DC: United States Department of Agriculture, Natural Resources Conservation Service; 2014.

Tagar AA, Changying J, Qishuo D, Adamowski J, Malard J, Eltoum AF. Implications of variability in soil structures and physio-mechanical properties of soil after different failure patterns. Geoderma. 2016;261:124-32. https://doi.org/10.1016/j.geoderma.2015.07.003

United States Environmental Protection Agency - Usepa. SW-846 EPA Method 3052: microwave assisted acid digestion of siliceous and organically based matrices. In: Usepa Test methods for evaluating solid waste. 3rd ed. Washington, DC; 1996.

Wilson SG, Lambert JJ, Nanzyo M, Dahlgren RA. Soil genesis and mineralogy across a volcanic lithosequence. Geoderma. 2017;285:301-12. https://doi.org/10.1016/j.geoderma.2016.09.013

Wright SF, Green VS, Cavigelli MA. Glomalin in aggregate size classes from three different farming systems. Soil Till Res. 2007;94:546-9. https://doi.org/10.1016/j.still.2006.08.003

Zörb C, Senbayram M, Peiter E. Potassium in agriculture - status and perspectives. J Plant Physiol. 2014;171:656-69. https://doi.org/10.1016/j.jplph.2013.08.008